Bulletin of the Seismological Society of America, Vol. 95, No. 5, pp. 1928–1939, October 2005, doi: 10.1785/0120040210

Long-Period Pulses in Broadband Records of Near Earthquakes

by Jiří Zahradník and Axel Plešinger

Abstract Broadband records of weak local earthquakes occasionally exhibit long-period, pulselike signals, appearing exclusively on horizontal components. Such signals have been recorded at station Sergoula in the Corinth Gulf by Guralp CMG-3T (100-sec) and Wielandt-Streckeisen STS-2 (120-sec) instruments. The pulses can be perfectly matched by the instrumental responses to a small step of acceleration. Similar pulses, observed during moderate near earthquakes at stations of the Greek National Network equipped with Lennartz Le-3D/20s (20-sec) sensors, can be explained in the same way. Numerical simulation of the pulses allows their removal, thus making the records fully utilizable for waveform inversion in seismic source studies. Prerequisite for that is precise knowledge of the instrument transfer function. We found that poles and zeros of the CMG-3T and STS-2 sensors were consistent with those given by the manufacturer, whereas those of the LE-3D/20s were not. We identified the latter by inversion of spontaneous pulses incidentally appearing in LE-3D/20s records without relation to any earthquake. What actually generates the earthquake-related horizontal acceleration steps remains unclear. Rapid and permanently lasting tilt is a very likely candidate. When we numerically model a coseismic near-field static displacement, we actually find a tilt step, but its amplitude is several orders below the observed values. We therefore rather speculate that it is a very local tilt, triggered by high-frequency ground vibrations.

Introduction

Since 1997, the Charles University Prague and the University of Patras have jointly operated several seismic stations in Greece. Each station is equipped with a Guralp broadband (0.02–100 sec) CMG-3T velocigraph and a Guralp strong-motion CMG-5T accelerograph. For technical and other reasons, the recording sites have been changed several times. The present network configuration and the available data are described at http://seis30.karlov.mff.cuni.cz. The data have been used in studies of significant regional events, for example, the 1999 Athens and Izmit earthquakes, the 2001 Skyros earthquake, the 2001 Egion sequence, and the 2003 Lefkada earthquake (Tselentis and Zahradník, 2000; Novotný *et al.*, 2001; Plicka and Zahradník, 2002; Zahradník, 2002; Zahradník *et al.*, 2004, 2005).

CMG-3T velocigrams of weak near earthquakes (local magnitude, ~1 to 3; epicentral distance ~1 to 10 km) occasionally, that is, not always, contain transient disturbances in the form of apparently one-sided pulses lasting about 100 sec. The pulses appear exclusively on the horizontal components, and their onset coincides with the *S*-wave onset. They occur well below the clip level of the instrument. The corresponding asymptotic signal in the mass-position channel, representing the integral of the velocity-proportional broadband output, is a permanent step. First observations of this phenomenon were reported soon after installation of the stations (Zahradník and Tselentis, 1999; Zahradník *et al.*, 2001). Since then it has been observed more or less regularly at all recording sites (Zahradník, 2004). It was not clear until recently whether the phenomenon was of natural origin or caused by instrumental malfunction.

To find the answer, we analyzed in this study long-period pulses (transients or disturbances, for short) recorded by several instruments at several stations. At the Sergoula station in the Corinth Gulf, a Wielandt-Streckeisen STS-2 (120-sec) instrument was temporarily deployed alongside the basic Guralp CMG-3T. Moreover, Lennartz Le-3D/20s (0.02–20 sec) velocigrams from several stations in Greece operated by the National Observatory of Athens (NOA) were analyzed. We show that the transients in all records can be perfectly explained as instrument responses to a steplike change of horizontal ground acceleration. All studied instruments behave qualitatively in the same way, but the disturbances have a different shape, reflecting the different transfer functions of the sensors. In this sense, the disturbances may serve as a natural calibration tool.

Various disturbances on horizontal components have been discussed in the literature. For instance, Dewey and Byerly (1969) summarized intensive discussions on tilt, accompanying the beginnings of seismometry. Hordejuk (1967) showed that rapid, steplike as well as deltalike

changes of tilt could occur during seismic shocks in epicentral regions (especially in mines) on the basis of observations by passive inertial seismographs with mechanical and galvanometric recording. Using modern broadband velocigraphs, Wielandt and Forbriger (1999) discovered and successfully extracted a tilt disturbance during weak volcanic earthquakes associated with coseismic strain in the epicentral region. In that case, the tilt was not a steplike change, but its temporal variation was similar to the vertical component of the vibratory seismic motion. Using accelerographs, Boore *et al.* (2002) analyzed baseline problems equivalent to the steplike acceleration change associated with strong ground motions. They speculated that they might be explained in terms of digitizer problems or hysteresis in the sensor, or in terms of the tilt, possibly including even a very local tilt due to slumping or cracking at the recording site.

In this study we demonstrate that horizontal acceleration steps can be associated as well with weak ground motions. The corresponding long-period transient disturbances on broadband velocigrams may produce serious difficulties in seismic source studies based on data from local and regional networks. Modeling and removal of these disturbances is therefore the main objective of this article.

Tilt, Acceleration Step, and Instrumental Response

Obviously, an inertial seismometer can be excited in the same manner as by a steplike change of ground acceleration for a variety of reasons, among others by spontaneous electrical or mechanical excitation similar to that commonly used in laboratory or onsite calibration tests. It can be injected in whatever component, horizontal or vertical. A specific case of the acceleration step is that occurring exclusively on horizontal components due to tilt.

Assume that an instrument is tilted by $\Theta(t)$, where Θ is the tilt angle between the instrument base and the horizontal plane, and t is the time. Consequently, the pendulum motion is affected by the horizontal component of the acceleration of gravity g, that is, $g \operatorname{tg} \Theta(t) \approx g\,\Theta(t) = a_{\text{tilt}}(t)$. When the tilt accompanies an earthquake, this additional horizontal acceleration due to tilt, $a_{\text{tilt}}(t)$, is superimposed on the horizontal seismic acceleration, $a_h(t)$. The vertical (Z-) component remains unaffected by the tilt, that is, it is subjected to the seismic acceleration $a_v(t)$ only. Wielandt and Forbriger (1999) assumed that the earthquake-related tilt angle $\Theta(t)$ is proportional to the Z-component record of $a_v(t)$, and, based on this assumption, they successfully decomposed observed waveforms into the tilt and seismic components. The assumption about proportionality between $\Theta(t)$ and $a_v(t)$ may be a reasonable approximation in the case that the tilt is transient, ceasing after the vibrations, that is, the ground returns to its previous position.

As shown later, the long-period transients analyzed in this article require another functional form of the acceleration time variation. Specifically, forward modeling of the instrument response revealed that the observed long-period disturbances have been caused by a rapid step change of the input horizontal acceleration. Mathematically, the appropriate approximation is the Heaviside function, $A\,H(t - t_0)$, where A is the amplitude of the acceleration step and t_0 is the onset time of the step. If the acceleration step occurs (not necessarily) due to tilt, then $\Theta(t) = a_{\text{tilt}}(t)/g = (A/g)H(t - t_0)$, that is, $\Theta(t)$ is also given by the Heaviside function, which means that the ground remains in the tilted position permanently.

For tutorial reasons, let us ignore the upper corner frequency of the instrument response and begin from the case of an accelerograph, for example, CMG-5T. Its response to input acceleration is flat down to zero frequency. Therefore, this instrument would record an instantaneous input step as a step, without any distortion, as shown in Figure 1a. This indeed had been the case with the strong-motion acceleration steps analyzed by Boore *et al.* (2002). However, during weak ground motions, the acceleration step (e.g., that related to the tilt) can be below the instrumental noise of the accelerograph, so neither the acceleration traces nor the integrated velocities provide reliable evidence of a small step.

Let us now consider a broadband velocigraph, for example, CMG-3T, whose long-period instrumental noise is lower than that of the CMG-5T. Its response to input velocity is flat for $f > f_0$, where f_0 is the lower cutoff frequency of the instrument's frequency response. The input acceleration step is equivalent to linearly growing input velocity (infinitely long-lasting ramp). As a result of the frequency-response falloff for $f < f_0$, the velocity ramp will be recorded with severe distortion, as in Figure 1b. This is not any malfunction but just the normal response of the instrument. The CMG-3T will record a long, apparently one-sided pulse of duration $T_0 \sim f_0^{-1}$ (in fact, the response is slightly two-sided, with a very small negative overshoot caused by the undercritical, 70% effective damping of the feedback system).

The terms "instantaneous" acceleration step or "infinitely long-lasting" velocity ramp have just a relative meaning. "Instantaneous" means that the rise time of the step is much shorter than T_0, and "infinitely long-lasting" means that the ramp is much longer than T_0. If these conditions are met, the differences compared with theoretical assumptions (zero rise time of acceleration step, infinite velocity ramp) are negligible. To demonstrate this, Figure 1c shows the response to an acceleration step with a rise time of 20 sec. The shape of the instrument response remains almost unaffected.

We thus face an interesting situation. The accelerograph does not distort the acceleration step. The broadband velocigraph distorts the linearly growing velocity ramp severely; that is, its output time history is far from being proportional to the input. Nevertheless, the velocigraph is much more appropriate for the detection of weak acceleration steps than the accelerograph because of its lower intrinsic long-period noise. That is why we later in this article do not discuss any records from the CMG-5T accelerographs, although they were collocated with the CMG-3T velocigraphs.

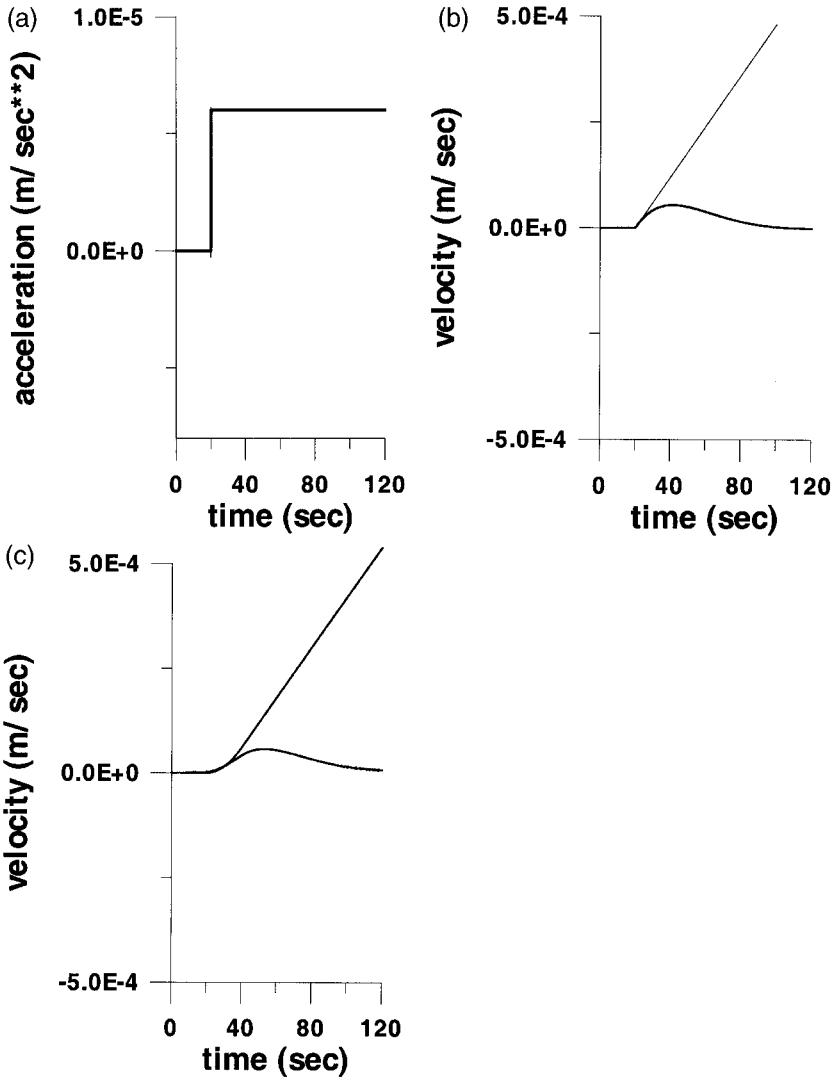

Figure 1. (a) Input acceleration (step) and theoretical output of the CMG-5T accelerograph. The two curves are almost identical; no difference can be seen. (b) Input velocity (linear ramp) and theoretical output of the CMG-3T velocigraph. The velocity ramp in this figure is equivalent to the step of input acceleration in Figure 1a. (c) As in Figure 1b, but an acceleration step with finite rise time.

Earthquake-Related Disturbances, CMG-3T and STS-2, SER Station

Let us now demonstrate a typical example of the observed long-period disturbance and check the plausibility of the above explanation. We start at the site where such disturbances have been occurring since 1997. This is station SER, situated in the small, almost uninhabited village of Sergoula, in the mountains on the northern side of the Corinth Gulf. The site geology is limestone. The installation is primitive: the instruments are deployed on the ground floor of a small one-story unused school building. Among hundreds of weak local events (magnitude, ~1 to 3; epicentral distance, ~1 to 10 km) recorded per month at SER, some two to five are disturbed.

An example of a typical disturbance on an unfiltered CMG-3T velocigram is shown in Figure 2a. It accompanied a small local earthquake, event 1 of Table 1, epicentral distance, 8 km. The disturbance is clearly visible on the east–west component. If we filter out frequencies $f > 1$ Hz, we can see it better, and a similar (but three times weaker) disturbance becomes evident also on the north–south component; see the top traces in Figure 2b. The onsets of the long-period transients on the horizontal components coincide with the onset of the *S*-wave group, see Figure 2c, and no disturbance is present on the vertical component (Fig. 2b).

To explain the disturbance, we return to the previous section. We assume an input acceleration step in the form of $A\ H(t - t_0)$, with $A = 1$, $t_0 = 0$, make the forward calculation of the CMG-3T velocity response (using the manufacturer's poles and zeros), and match the record by adjusting the two free parameters, t_0 and A, using amplitude scaling and trial-and-error time shifting. As result, the observed disturbance on the SER record is simulated very well; see the bottom traces in Figure 2b. The resulting horizontal acceleration step, appropriate for this case, is $A = 2 \times 10^{-6}$ m/sec^2 and 6×10^{-6} m/sec^2 for the north–south and east–west component, respectively (Table 2).

To confirm this explanation, another broadband sensor (an STS-2) was temporarily installed at the SER station. A

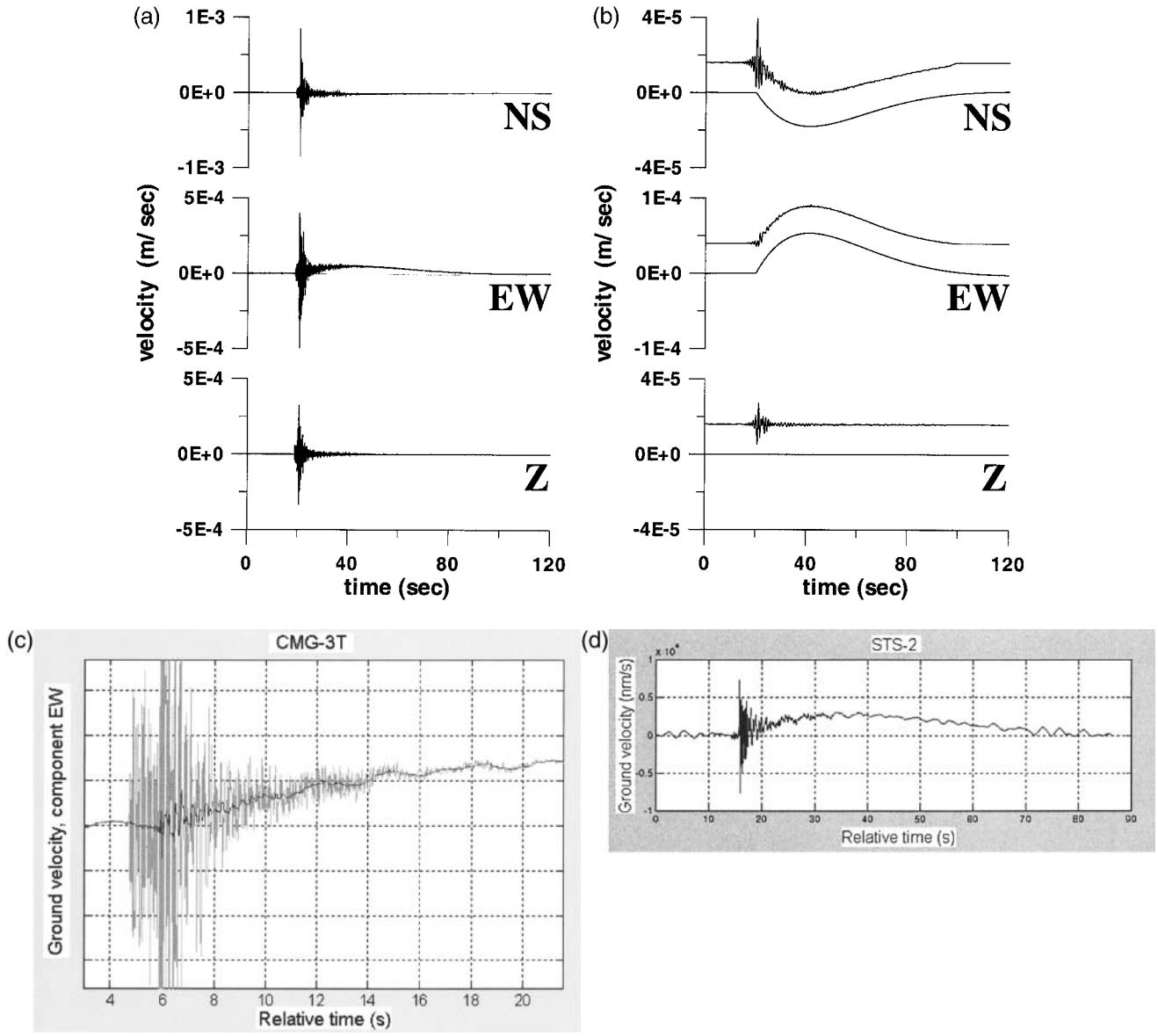

Figure 2. (a) Example of an unfiltered velocity record (CMG-3T) with a strong long-period disturbance on the east–west component. Event 1, station SER. (b) Top traces: 1-Hz low-pass filtered record of Figure 2a; the long-period disturbances are visible on both horizontal components. Bottom traces: CMG-3T response to acceleration steps $A = 2.0 \times 10^{-6}$ m/sec^2 and 6.1×10^{-6} m/sec^2 applied to the north–south and east–west component, respectively. (c) Unfiltered (gray) and 3-Hz-low-pass filtered (black) CMG-3T velocigram. Event 1, station SER, component east–west. The onset of the long-period disturbance coincides with that of the *S*-phase of the earthquake signal. (d) 1.5-Hz low-pass filtered STS-2 velocigram. Nonlocated near event, station SER, component east–west. The onset of the long-period disturbance coincides with that of the *S* phase of the earthquake signal.

timing problem in the data logger did not allow us unambiguously to assign the earthquakes recorded to those of the CMG-3T. Nevertheless, without any doubt, in two of the over 300 recorded local events, quite analogous long-period disturbances, although of smaller amplitude, were evident. An example is shown in Figure 2d.

Earthquake-Related Disturbance, Le-3D/20s, ATH (NOA) Station

Strange long-period pulses have also been known to appear in records of the broadband stations of the Greek national network, operated by NOA, the National Observatory

Table 1
Parameters of the Studied Events

Event	Local Magnitude	Date	Origin Time (h:m, utc)	Latitude (deg, N)	Longitude (deg, E)
1 (PATNET)	3.2	13 Nov. 2002	21:55	38.37	21.99
2 (NOA)	4.4	18 June 2003	05:25	38.62	23.68
3	X	26 Apr. 2004	13:21	X	X
4 (NOA)	5.3	2 Dec. 2002	04:58	37.80	21.15

The locating organization is indicated in the first column. Event 3 is a spontaneous long-period pulse not connected to any earthquake.

Table 2
Seismic Stations Used

Station	Latitude (deg, N)	Longitude (deg, E)	Event	Epicentral Distance (km)	Acceleration Step (m/sec^2)
SER	38.41	22.06	1	8	NS: 2.0×10^{-6}
					EW: 6.1×10^{-6}
ATH	37.97	23.72	2	72	NS: 1.9×10^{-4}
SMG	37.71	26.84	3	X	NS: 1.6×10^{-3}
					EW: 1.2×10^{-3}
RLS	38.06	21.47	4	40	NS: 6.0×10^{-4}
					EW: 6.0×10^{-4}

The event numbers refer to Table 1. Event 3 is a spontaneous long-period pulse not connected to any earthquake. The acceleration step is retrieved in this article.

of Athens (N. Melis and E. Sokos, personal comm., 2004). Most of the broadband instruments of the NOA network are Lennartz Le-3D/20s sensors.

As an example, Figure 3a shows the record of the Psachna earthquake, recorded at the ATH station, epicentral distance 72 km (Tables 1 and 2). In the north–south component of the velocigram, although not very pronounced, a long-period disturbance can be seen. In the integrated velocigram, that is, the record of ground displacement without instrumental correction (Fig. 3b), the disturbance on the north–south component becomes very clear. The shorter duration of the long-period pulse in comparison with those on the horizontal CMG-3T and STS-2 records is due to the shorter effective free period of the Le-3D/20s sensor (20 sec instead of 100 or 120 sec, respectively). To explain the present example, we must discuss the Le-3D/20s transfer function in greater detail.

Spontaneous Disturbance at Station SMG (NOA) and Recalibration of the Le-3D/20s Sensor

The manufacturer of Le-3D/20s sensors strongly warns against their use for periods $T > 20$ sec, where the transfer function allegedly may fall off very steeply (D. Stoll, personal comm., 1999). For $T < 20$ sec, the manufacturer recommends the use of the transfer function of an optimally damped 20-sec standard-class seismometer. We show below that this may lead to quite erroneous interpretations and that the actual transfer function, even for periods $T > 20$ sec, can be retrieved from routine recordings.

From time to time, Le-3D/20s records contain large long-period pulses not related to any earthquake. An example is shown on the top traces of Figure 4. This incidental observation comes from the SMG station on Samos Island (Tables 1 and 2, event 3). In this case the amplitudes on the north–south and east–west components were two orders of magnitude larger than the noise amplitude before and after the pulses. That is why, in the adopted scale, the traces before and after the north–south and east–west pulses look like a straight line. The Z component is completely free of any disturbance, and it contains only seismic noise. The cause of such spontaneous pulses on the horizontal components is puzzling. Absence of earthquake motion makes the tilt explanation less likely, although not impossible. We shall return to this question in our conclusions. Nevertheless, whatever the cause of the pulses is, their shape strongly suggests that they represent the instrument response to an acceleration step or, in instrumental terminology, its release-test response.

Therefore, we use the observed disturbances as in the standard release-test calibration, calculate the transfer function, and *a posteriori* validate the poles and zeros through successful modeling of the other long-period transients. The transfer function is obtained by inversion of the observed pulses into the instrumental parameters using the system identification code UNICALT (Plešinger, 1998). The inversion yields a third-order velocity transfer function; the retrieved zeros and poles are given in Table 3. Figure 4 compares the observed and modeled pulse shapes, which prove a very good match. The appropriate amplitude of the input acceleration steps is 1.6×10^{-3} and 1.2×10^{-3} m/sec^2 on the north–south and east–west component, respectively.

Figure 5 shows the modulus of the resulting Le-3D/20s transfer function for input velocity in comparison with that of the velocity transfer function of a standard-class 20-sec seismometer (or a 20-sec force-balance seismometer with integral feedback). The difference in the asymptotic low-frequency slope, actually f^3 (18 dB/octave) instead of f^2 (12 dB/octave), is crucial and must not be neglected in the interpretation of Le-3D/20s recordings of seismic signals with periods longer than, say, 10 sec.

Knowledge of the actual poles and zeros opens the way

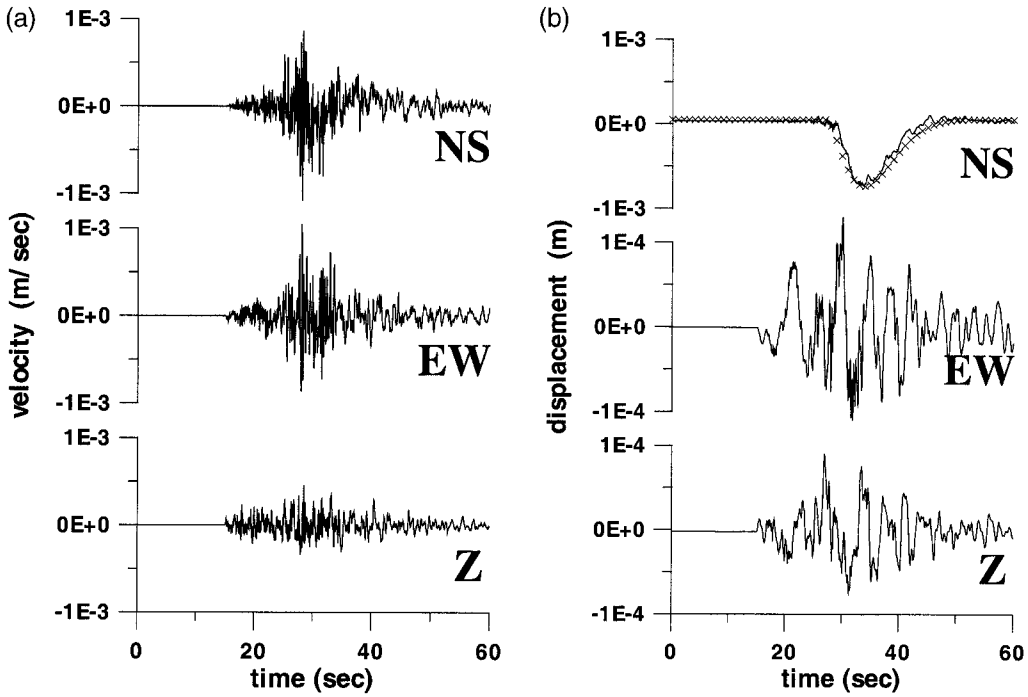

Figure 3. (a) Example of an unfiltered velocity record (Le-3D/20s) with apparently weak long-period disturbance on the north–south component. Event 2, station ATH. (b) Record of Figure 3a transformed to displacement. The long-period disturbance on the north–south component is very large (note the amplitude scales). The trace (shown by crosses) superimposed on the recorded north–south component is the Le-3D/20s response calculated for an acceleration step of $A = 1.9 \times 10^{-4}$ m/sec^2.

toward correcting NOA records spoiled by the long-period disturbances. In fact, recalibration should be performed separately for each instrument, but we can show that the values in Table 3, derived from the SMG records, are (approximately) valid also for the other stations. First, we return to the previous case of the Psachna earthquake recorded at the ATH station, shown in Figure 3b. Adopting the instrumental parameters of Table 3, we get a satisfactory simulation of the long-period disturbance on the north–south component. The displacement pulse is fitted by the Le-3D/20s response corresponding to an input acceleration step of $A = 1.9 \times 10^{-4}$ m/sec^2. The fact that the east–west component is free of any long-period transient indicates that this case has nothing to do with tilt, leaving space for speculations about an unknown electronic or mechanical intrinsic disturbance. This, however, goes beyond the scope of this article.

Earthquake-Related Disturbance and Its Removal: Le-3D/20s, RLS (NOA) Station

Finally, we study an event where the long-period disturbance is completely masked in the velocity record by stronger short-period waves (Fig. 6a). It is the case of the Vartholomio earthquake (event 4 in Table 1), recorded at an epicentral distance of 40 km at the RLS station (Table 2).

To demonstrate the RLS problem more clearly, let us again transform the velocity to displacement, without any filtering. The long-period disturbance appears now on both horizontal components (Fig. 6b). The *Z* component is a normal seismic motion, without any disturbance. This case stimulated two tasks: (1) to prove once more the explanation in terms of the assumed acceleration step, using the instrument parameters retrieved from another event at another station (Table 3), and (2) to remove the disturbance, thus providing a reconstructed record usable in seismic-source studies.

Task (1) is solved in Figure 6b (bottom traces). It shows that the long-period displacement disturbance is perfectly matched by the instrument output corresponding to the poles and zeros in Table 3 and to an input acceleration step of 6×10^{-4} m/sec^2 for both the north–south and east–west components. Task (2) is solved in Figure 6c, where the synthetic disturbance from step (1) is subtracted from the record. The resulting record has no more anomalous features, as shown below.

Before proving that in Figure 6c we already have a normal seismic record, it might be instructive to explain how the long-period problem was detected. It appeared when we tried to include the RLS record in the moment tensor inversion. The record was integrated to displacement, and, in contrast to the above record in Figure 6b, it was bandpass filtered in the period range of 10 to 20 sec. In this band, the disturbance is not obvious at first glance, and, as such, it is very dangerous, particularly for any automated processing. Therefore, when the RLS record was used (together with

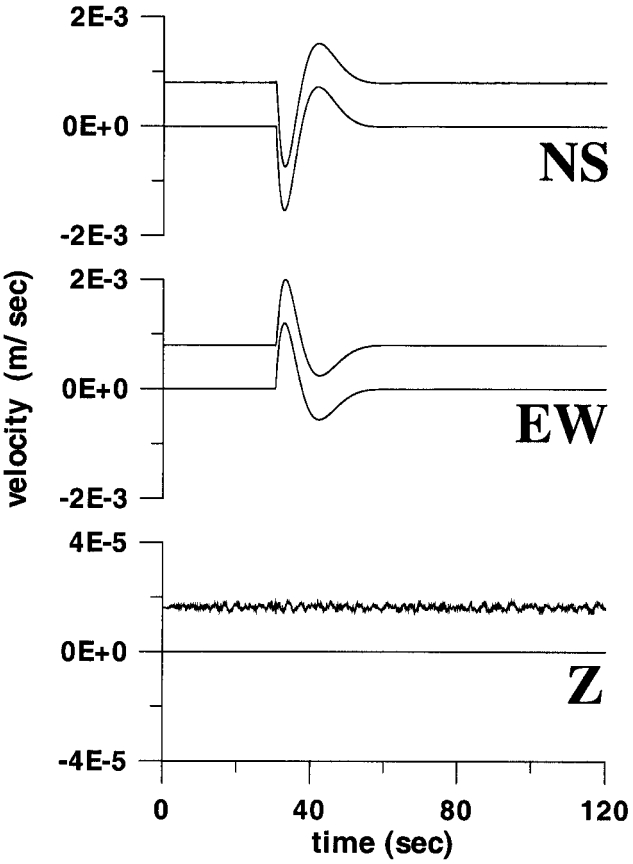

Figure 4. Top traces: unfiltered velocity record (Le-3D/20s) with very large disturbances on both horizontal components not linked to any earthquake. Note the amplitude scales. These spontaneous disturbances serve as a natural calibration pulses providing the instrumental parameters (Table 3). Bottom traces below north–south and east–west: Le-3D/20s responses to acceleration steps of $A = 1.6 \times 10^{-3}$ and 1.2×10^{-3} m/sec^2, respectively. Event 3, station SMG.

Table 3
Le-3D/20-sec Sensor Parameters Retrieved

East–West Component		North–South Component	
Real Part	Imaginary Part	Real Part	Imaginary Part
Poles (rad/sec)		Poles (rad/sec)	
−0.2192	0.2384	−0.2232	0.2318
−0.2192	−0.2384	−0.2232	−0.2318
−0.1973	0.0000	−0.2289	0.0000

The transfer function for velocity input has three zeros in the origin of the complex plane (values 0, not shown for brevity). The normalization factor equals 1.0.

four other regional records), it provided a moment tensor solution completely different from the other published solutions, for example, that of MEDNET. As a next step, instead of continuing in the inversion, we used the source parameters of MEDNET, solved a forward problem, and

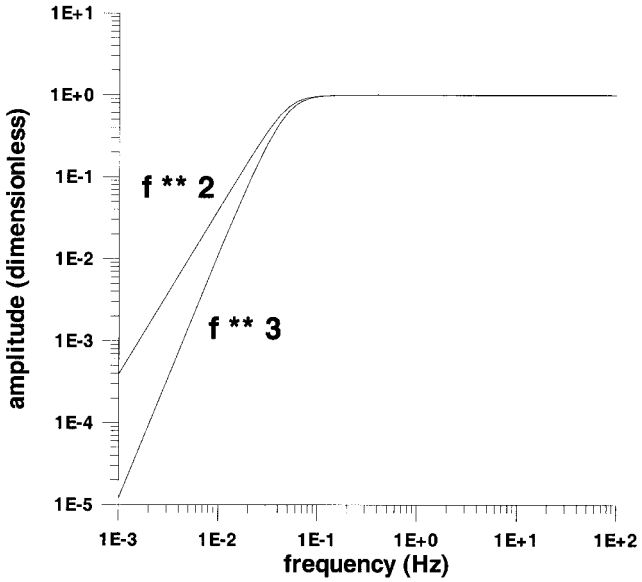

Figure 5. Modulus of the identified third-order Le-3D/20s transfer function (steady-state amplitude-frequency response for input velocity) compared with that of a second-order transfer function typical for a 20-sec standard-class seismometer or for a 20-sec force-balance seismometer with integral feedback.

compared the records with the synthetics. Details of the modeling, such as the crustal model, focal mechanism, and so on, unimportant here, can be found in the next section. A very bad agreement between the recorded and synthetic waveforms indicated that there had to be something wrong with the RLS record (Fig. 7a).

The general lesson learned is that prior to any regional broadband waveform inversion, it is very useful to check the unfiltered displacement records not corrected for the instrument response, and to compare the bandpass-filtered, instrumentally corrected displacement records with the synthetics calculated with any (preliminary) available focal mechanism solution. This check may detect records affected by long-period disturbances that are visually not obvious but may destroy the source inversion.

Returning to Figure 6c to prove that we already have a normal seismic record, we check the reconstructed RLS record (after removal of the long-period disturbance) against the forward solution with the MEDNET source parameters. This is done in Figure 7b, showing that the reconstructed RLS waveforms are a fairly good fit with the synthetics, substantially better than before the reconstruction (in Fig. 7a). This means that, in contrast to the original RLS record, the resulting reconstructed RLS record is already suitable for source studies. Such a study will be presented in a separate article.

It might appear too laborious to deal with one station so much, and perhaps even unnecessary when the other stations provide good records, but we must underline the im-

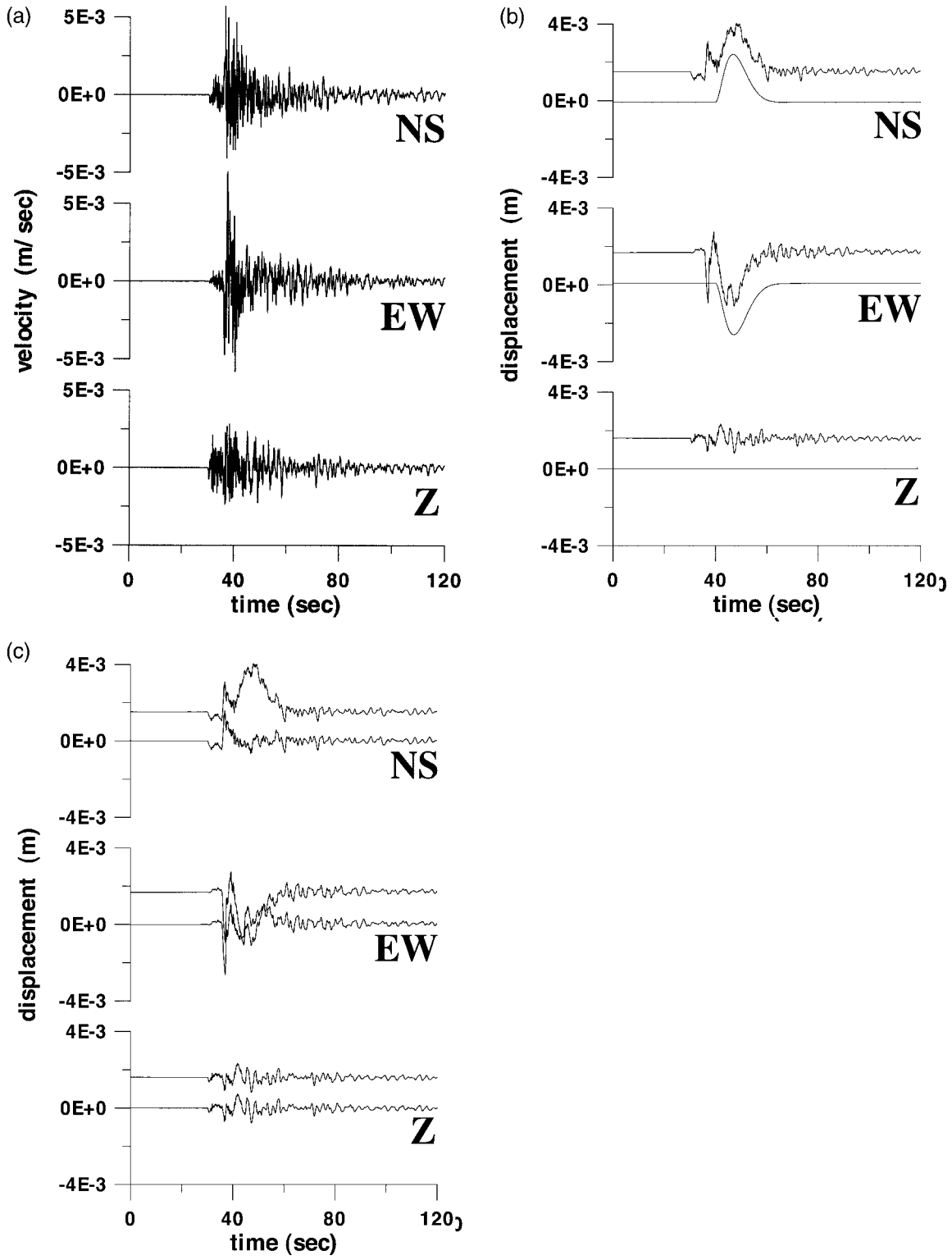

Figure 6. (a) Example of an unfiltered velocity record (Le-3D/20s) with a long-period disturbance on both horizontal components, masked by the short period waves. Event 4, station RLS. (b) Top traces: record of Figure 6a transformed to displacement. The long-period disturbances on both horizontal components are very large (note the amplitude scales). Bottom traces: Le-3D/20s response to an acceleration step of $A = 6.0 \times 10^{-4}$ m/sec^2 applied to the north–south and east–west components. (c) Top traces: same as in Figure 6b. Bottom traces: reconstructed record obtained by subtracting the simulated disturbance (difference between top and bottom traces of Fig. 6b).

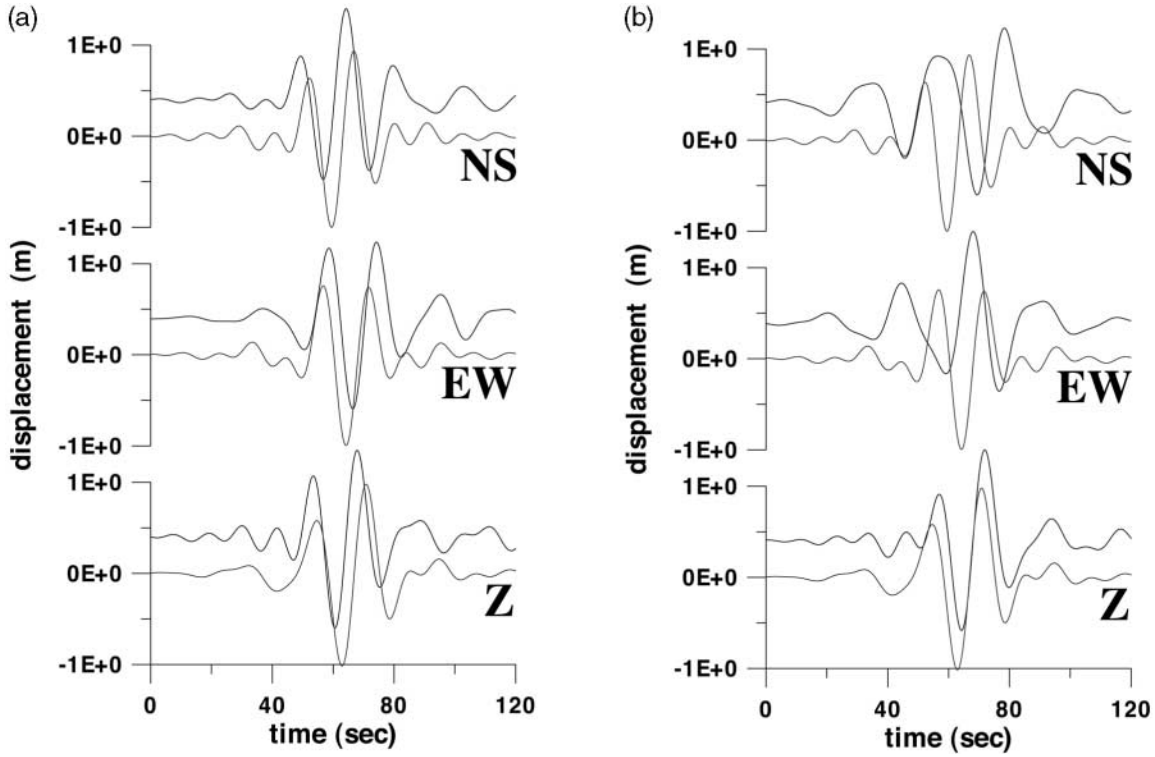

Figure 7. (a) Top traces: displacement record of Figure 6b, 10- to 20-sec bandpass-filtered, instrumentally corrected, and normalized to unit amplitude. Bottom traces: synthetic seismograms calculated for the fault-plane solution reported by MEDNET. Due to the long-period disturbance present in the recorded north–south and east–west components, there is a very poor match with the synthetics. (b) Top traces: record of Figure 7a after removal of the disturbance from the north–south and east–west components. Bottom traces: same synthetics as in Figure 7a. Note that compared to Figure 7a, the match is substantially better.

portance of the reconstruction of the RLS record because RLS was the nearest broadband station that recorded the significant M 5.3 Vartholomio earthquake. Therefore, we offer the reconstructed RLS record in digital form, upon request.

Quantitative Estimate of the Coseismic Strain and Tilt

Is it possible to explain the inferred amplitudes of the acceleration steps in terms of coseismic strain and tilt? Let us consider the permanent coseismic displacement (i.e., the resulting static offset after cessation of the vibrations), existing close to an earthquake source, and mathematically described by near-field terms of the Green's function. Denote by d_v the vertical component of the final static displacement. It is a function of the space coordinates, d_v (x,y), and its gradient at a station $(\partial d_v/\partial x, \partial d_v/\partial y)$ represents the tilt angles Θ for the north–south and east–west component, respectively. Then, as already explained previously, multiplication by g yields the acceleration step amplitude A. An order-of-magnitude estimation of this effect will show how large the amplitude can be, and whether it explains the observed values (Table 2).

The near-field displacement is simulated for the RLS station, and the Vartholomio earthquake (event 4) by using the discrete wavenumber method of Bouchon (1981) and Coutant (1989). We use the 1D stratified crustal model of Haslinger *et al.* (1999). The point-source depth and epicentral distance are 20 km and 40 km, respectively. The focal mechanism, represented by strike $= 302°$, dip $= 85°$, and rake $= -10°$, is taken from the MEDNET agency. Slip at the source is represented by the Heaviside function, with scalar moment $M_o = 2.9 \times 10^{17}$ Nm. We study the frequency band from 0 to 0.1 Hz (tapered up to 1.0 Hz), but the permanent displacement is independent of this particular choice. To evaluate the tilt, we take the vertical component of the complete wavefield at two points, 1 and 2, separated by a base of length L, and calculate the finite difference $\Theta(t) = (d_v^1 - d_v^2)/L$. One of the two points is the RLS station, while the other point is located toward north–south or east–west, at a distance of $L = 100$ or 200 m. The order-of-magnitude estimation of the tilt size is independent of the particular choice. A typical example is presented in Figure

8a, where the static offset of the $\Theta(t)$ trace is of the order of 2×10^{-8} (dimensionless). When multiplied by g, we get a synthetic simulation of the tilt-related acceleration; thus, the acceleration step amplitude is $A = 2 \times 10^{-7}$ m/sec^2. Figure 8b depicts also the integrated trace. When multiplied by g, it is the tilt-related velocity, clearly showing the linear ramp, as required to explain the long-period disturbances on the broadband velocigrams, as discussed previously. This experiment proves that coseismic permanent tilt may exist at the RLS station, but (in the studied case) it strongly underestimates the observed value of A. Indeed, comparing with Table 2, we see that for the RLS station the present estimate of A is three orders of magnitude below the observed value. We can perhaps speculate about uncertainty in the considered source depth, focal mechanism, and so on, but perturbations of the parameters will not increase the theoretical estimate by more than one order of magnitude.

Regarding the SER station, event 1, we have a closer source and smaller magnitude. Table 2 gives a typical value of A of the order of 1×10^{-6} m/sec^2, but the theoretical estimate is again a few orders of magnitude below the observed value. These estimates are in general agreement with direct strain and tilt measurements at the Corinth Rift Laboratory on Trizonia Island (P. Bernard, personal comm., 2004), where the observed coseismic strains have not exceeded 1×10^{-8}, but very local tilts reached 1×10^{-7}.

Some Qualitative Speculations about the Acceleration Steps

Although all the long-period transients presented above could be explained as steplike changes in horizontal acceleration, their origin most likely was not the same. This is indicated not only by the different amplitude of the inferred acceleration step but also by the other circumstances: events 1 and 4 had earthquake-related disturbances on both horizontal components; event 2 had a disturbance only on the north–south component; and event 3 was not related to any earthquake. This means that events 1 and 4 are candidates for explanation in terms of tilt but, as shown in the previous paragraph, coseismic regional tilt seems to be too small.

In such a situation, the simplest explanation of the records disturbed in both horizontal components is a very local tilt (tilt on a very small spatial scale). For the following, let d_v^1 and d_v^2 denote a small permanent vertical displacement of unknown origin, existing over a base length L, without any direct relation to the near-field effect of the seismic source. Then, the estimate of $\Theta = (d_v^1 - d_v^2)/L$ can be increased with an arbitrary nonzero value of the differential offset $(d_v^1 - d_v^2)$, just by decreasing L. The smallest reasonable value of the base length L is the distance between the seismometer feet, that is, 1×10^{-1} m. Then, even the largest values in Table 2, those of $A = 1 \times 10^{-3}$ m/sec^2, $\Theta =$

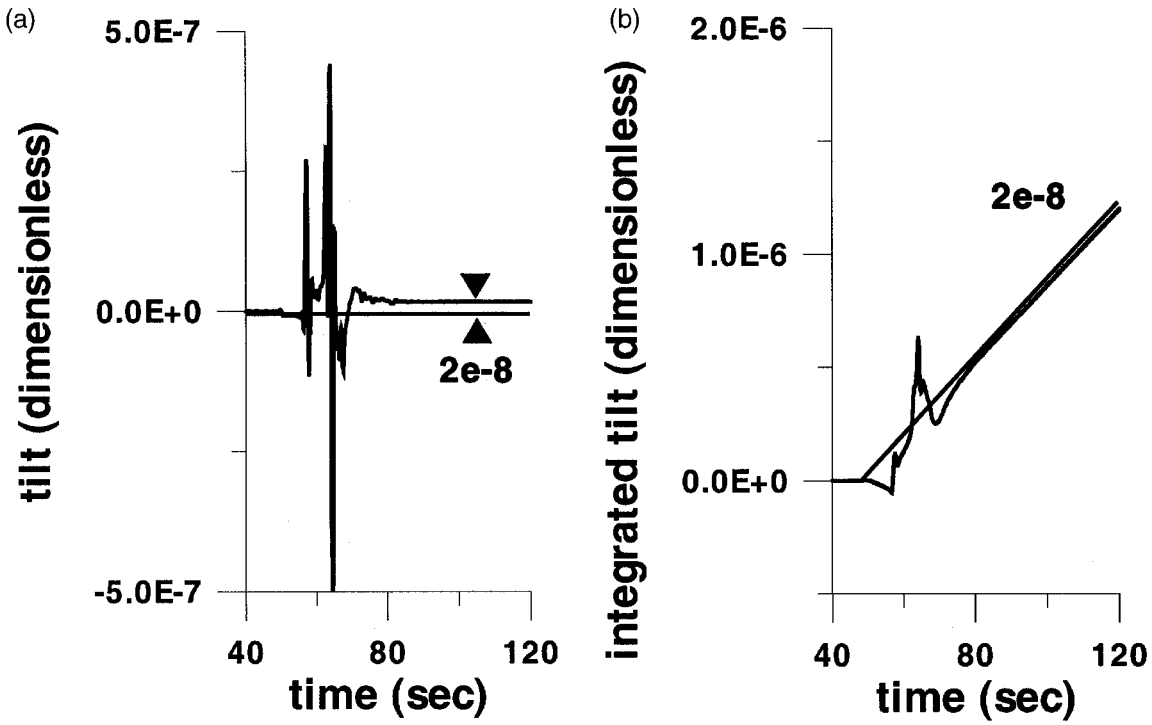

Figure 8. (a) Theoretical time variation of the tilt obtained by numerical differentiation of the synthetic seismograms. Note the permanent (2×10^{-8}) tilt after passage of the vibratory motion. (b) Same as in Figure 8a, but numerically integrated. The linear slope corresponds to the static offset in Figure 8a. Comparison with Figures 1b and 1c proves that the coseismic tilt might produce long-period disturbances, but the tilt amplitude in the studied case is too low to explain the observations.

1×10^{-4}, can be explained by $(d_v^1 - d_v^2) = 1 \times 10^{-5}$ m. Such a value can be easily accepted, because it can occur in many possible ways, for example, because of cracks of microscopic material (dust) particles below the seismometer feet. In connection with similar disturbances observed on records of the Kirnos seismographs, carefully installed in the vault of the permanent seismic station Praha in a seismically quiet region of the former Czechoslovakia, this idea was suggested many years ago by J. Janský (personal comm., 1975). There are, of course many other possibilities for getting the observed order of magnitude of A with various combinations of $(d_v^1 - d_v^2)$ and L. For example, we can postulate a microscopic crack in the construction material of the pillar or in the underlying block of rock, with $(d_v^1 - d_v^2) = 1 \times 10^{-4}$ m and $L = 1$ m, respectively. Certain microeffects might also happen inside the seismometer itself.

Some of these effects do not even require any earthquake triggering, since the disturbance can appear just because of temperature changes, effects of water, mechanical microeffects, and so on. This may be the case with event 3 at the SMG station, with the largest observed acceleration step not related to any earthquake, or with event 2 at the ATH station, where only the north–south component was affected. An electronic problem leaving one or two components unaffected seems unlikely, since such effects usually cohere with the power supply and appear therefore simultaneously on all components.

On the other hand, the observations from the Sergoula station, where hundreds of local events are recorded every month and the nearest of which produce long-period disturbances corresponding to a steplike change in the horizontal acceleration almost systematically, represent a good possibility that a very local (short-base) tilt is provoked by seismic motion. In particular, the very rich, high-frequency content of the involved seismic motions seems to play an important triggering role. To learn whether this is specific just for the Sergoula recording site, and to get more information about the spatial scale (short-base, local, wider than local) of the phenomenon, further simultaneous observations with at least two very broadband instruments (preferably STS-2) installed under different conditions (surface, subsurface) at several stations is envisaged. Placing a CMG-3T and STS-2 on a common base, sitting on three feet like a single seismometer (Ch. R. Hutt, personal comm., 2004), would be very desirable to check the coherency of the recordings. Preparatory works for experiments of both kinds are under way at the Sergoula station.

Conclusions

The horizontal components of weak ground motions recorded by broadband velocigraphs may contain long-period disturbances. This has been demonstrated for four recording sites in Greece and for three different types of instruments. Most of the disturbances are related to nearby earthquakes: they are superimposed on the earthquake signal and start at the onset of the S wave. Less frequently, the disturbances can occur even without connection to any earthquake.

A typical disturbance has the form of a long, apparently one-sided pulse, whose exact shape depends on the type of instrument. We have shown that the disturbances represent the normal instrument response to a steplike acceleration time history, equivalent to an infinitely growing linear ramp of velocity. The steplike acceleration input has explained all the studied disturbances, independently of the recording site and instrument type. By steplike acceleration, we mean a sudden change from zero to some permanent value A (i.e., the Heaviside function). The words "sudden" and "permanent" have a relative meaning. For example, in case of the 100-sec velocigraph CMG-3T, it means an acceleration growing from 0 to A in much less than 100 sec, and lasting at A much more than 100 sec.

The disturbances can be modeled provided the instrument transfer function is known with adequate accuracy. For the CMG-3T and STS-2, modeling using the manufacturers' poles and zeros was successful. For the Le-3D/20s, we had to infer a new (third-order, see Table 3) approximation of the actual transfer function by identification of incidental strong pulses of unknown origin, which excited the instrument in the same way as a standard release test. We have calculated the acceleration-step amplitude A for a few typical examples of the disturbance (Table 2) and found values ranging from 1×10^{-3} to 1×10^{-6} m/sec^2. Once the value of A is known, the long-period disturbance can be numerically simulated and removed from the record.

Removal of the disturbances is of particular importance in case of regional (or local) source studies, when only a few stations are available so that each record has great significance. In this context, it is sometimes more important to detect a long-period disturbance than to remove it. The disturbances may be completely hidden in the velocigrams, that is, masked by stronger waves of shorter periods. Therefore, to detect them prior to any source inversion, it is useful to inspect unfiltered, full-band, instrumentally uncorrected displacement records, or to compare instrumentally corrected displacement records with forward simulation using any available (preliminary) source location and focal mechanism.

The simplest interpretation of the horizontal acceleration step is a tilt step, that is, the instrument base moves instantly from its original horizontal position to an inclined position, and remains in that new position. However, it is unclear where the tilt steps come from. A numerical example has shown that coseismic permanent displacement (the near-field static offset), and its spatial variability, can cause a tilt step of the required time variation. However, its size has been found to be several orders of magnitude below the A values retrieved from the observed disturbances given in Table 2. The most likely explanation is that the relatively large detected tilt is not due to coseismic (near-field) strain, but that it has a more local nature. We can easily accept the existence of a relatively large tilt due to a microscopic dif-

ferential vertical offset (e.g., 1×10^{-5} m) occurring over a very short base (e.g., 1×10^{-1} m), but we have no direct observational evidence for that. We can only speculate that earthquake-generated high-frequency ground vibrations may produce such a large local tilt by creating a small-scale material instability immediately below the instrument, below the station building, or in the underlying block of rock. Even other instabilities may play a role, such as thermally or chemically induced microcracks of the ground particles, and these do not necessarily require any excitation by an earthquake.

Acknowledgments

We gratefully acknowledge the constructive comments of Dr. Ch. R. Hutt (USGS Albuquerque Seismological Laboratory) and an anonymous reviewer. We thank Prof. G.-A. Tselentis, Director of the Seismological Laboratory, Patras University, for supporting the joint operation of the Charles University seismic stations in Greece. The Institute of Geodynamics, National Observatory of Athens, provided data from the Lennartz instruments. Thanks go to Dr. G. Stavrakakis, Director, as well as to Dr. N. Melis and Dr. E. Sokos. Instrumental and financial support for comparative STS-2 observations at the Sergoula station has been provided by the Geophysical Institute of the Czech Academy of Sciences and within project GACR 205/02/0381 coordinated by Dr. J. Horálek. We profited from discussions with Dr. P. Bernard, and we thank Dr. V. Janský, Dr. V. Plicka, Ing. P. Jedlička, and Dr. B. Růek for their technical and professional help. The work was financially supported from several projects in the Czech Republic, MSM 113200004 and GACR 205/03/1047, and from the EC project EVG3-CT-2002-80006 (MAGMA).

References

Boore, D. M., Ch. D. Stephens, and W. B. Joyner (2002). Comments on baseline correction of digital strong-motion data: examples from the 1999 Hector Mine, California, earthquake, *Bull. Seism. Soc. Am.* **92,** 1543–1560.

Bouchon, M. (1981). A simple method to calculate Green's functions for elastic layered media, *Bull. Seism. Soc. Am.* **71,** 959–971.

Coutant, O. (1989). Program of numerical simulation AXITRA, Research Report, LGIT, Grenoble.

Dewey, J., and P. Byerly (1969). The early history of seismometry (to 1900), *Bull. Seism. Soc. Am.* **59,** 183–227.

Haslinger, F., E. Kissling, J. Ansorge, D. Hatzfeld, E. Papadimitriou, V. Karakostas, K. Makropoulos, H.-G. Kahle, and Y. Peter (1999). 3D crustal structure from local earthquake tomography around the Gulf of Arta (Ionian region, NW Greece), *Tectonophysics* **304,** 201–218.

Hordejuk, J. (1967). An analysis of rapid changes of crustal tilts recorded by seismic instruments with mechanical and galvanometric recorders, *Publ. Inst. Geophys. Pol. Acad. Sci.* **67,** 141–148.

Novotný, O., J. Zahradník, and G-A. Tselentis (2001). Northwestern Turkey earthquakes and the crustal structure inferred from surface waves observed in the Corinth Gulf, Greece, *Bull. Seism. Soc. Am.* **91,** 875–879.

Plešinger, A. (1998). Determination of seismograph system transfer functions by inversion of transient and steady-state calibration responses, *Studia Geophys. et Geod.* **42,** 472–499.

Plicka, V., and J. Zahradník (2002). The use of eGf method for dissimilar focal mechanisms: the Athens 1999 earthquake, *Tectonophysics* **359,** 81–95.

Tselentis, G.-A., and J. Zahradník (2000). The Athens earthquake of 7 September 1999, *Bull. Seism. Soc. Am.* **90,** 1143–1160.

Wielandt, E., and T. Forbriger (1999). Near-field seismic displacement and tilt associated with the explosive activity of Stromboli, *Ann. di Geofis.* **42,** 407–416.

Zahradník, J. (2002). The weak-motion modeling the Skyros island, Aegean Sea, $M_w = 6.5$ earthquake of 26 July 2001, *Studia Geophys. et Geod.* **46,** 753–771.

Zahradník, J. (2004). How many seismographs do we need to record ground motion at a station?, *Studia Geophys. et Geod.* **48,** 483–492.

Zahradník, J., and G.-A. Tselentis (1999). Broadband Stations in Western Corinth Gulf. ORFEUS Electronic Newsletter, Vol. 1, No. 3, http://orfeus-eu.org/newsletter/vol1no3/index.html

Zahradník, J., J. Janský, and N. Papatsimpa (2001). Focal mechanisms of weak earthquakes from amplitude spectra and polarities, *Pure Appl. Geophys.* **158,** 647–665.

Zahradník, J., J. Janský, E. Sokos, A. Serpetsidaki, H. Lyon-Caen, and P. Papadimitriou (2004). Modeling the M_L 4.7 mainshock of the February–July 2001 earthquake sequence in Aegion, Greece, *J. Seism.* **8,** 247–257.

Zahradník, J., A. Serpetsidaki, E. Sokos, and G.-A. Tselentis (2005). Iterative deconvolution of regional waveforms and a double-event interpretation of the 2003 Lefkada earthquake, Greece, *Bull. Seism. Soc. Am.* **95,** 159–172.

Faculty of Mathematics and Physics
Charles University Prague
V Holesovickach 2
180 00, Prague 8, Czech Republic
jz@karel.troja.mff.cuni.cz
(J.Z.)

Geophysical Institute
Academy of Sciences of the Czech Republic
Bocni II/1401
141 31, Prague 4, Czech Republic
pless@ig.cas.cz
(A.P.)

Manuscript received 3 November 2004.